Kicker Magnet Modulator in the 2-GeV Pohang Light Source

S. H. Nam, *Member, IEEE,* and S. H. Jeong

***Abstract*—The 2.0-GeV Pohang Light Source (PLS) is a third-generation synchrotron light source that is the first such facility in Korea and the fifth in the world. The PLS mainly consisted of a full-energy injection linac and a storage ring. Four kicker magnets are installed in the storage ring tunnel to move the stored beam orbit in the storage ring closer to the injected beam from the beam transfer line. The injected beam then falls into the storage ring beam dynamic aperture. A kicker magnet modulator drives all four kicker magnets to maintain field balance and synchronized kick of the beam. Specification of the kicker magnet modulator is ∼6.0-μs-full width, 200-ns flattop width with ±0.2% regulation, ∼24-kA peak current, and 10-Hz repetition rate. Two thyratron switches (EEV CX-1536AX) are used in the system. As the inverse voltage is dangerous to thyratron operation, a new surge suppression circuit was developed. The kicker modulator has been operated very reliably since its installation in August 1995. In this article, design, simulation, and experimental results of the kicker magnet modulator are discussed. In addition, measurement result of spatial B-field distribution in the kicker magnet and maximum operating range of kicker magnet are discussed.**

***Index Terms*—Injection, kicker modulation.**

I. Introduction

THE Pohang Light Source (PLS) is a third-generation synchrotron radiation facility that is the first such facility in Korea, and the fifth in the world [1], [2]. The PLS consists of a 2-GeV electron injection linac and a storage ring. The 2-GeV electron beam from the linac is transported through a beam transfer line to the storage ring with an 8° vertical angle. The beam is then vertically deflected again to recover its horizontal path. The final deflection places the electron beam on the same level as the stored beam in the storage ring. The final deflection is done by a septum magnet. The injected beam is then placed within the storage ring beam dynamic aperture by kicker magnets. In Fig. 1, a concept of the bumped beam orbit is presented. A thin septum magnet wall initially separates the injected beam. A total of four kicker magnets (BMP1, 2, 3, and 4 in Fig. 1) are used to disturb the normal storage ring beam orbit, to move the orbit closer to the septum magnet wall, and to bring the injected beam within the storage ring beam dynamic aperture. A tune of PLS is about 1/4. The electron beam returns to approximately the same horizontal position where it is injected after four storage ring turns. Therefore, it is desirable to remove the kicker magnet modulator current within four revolutions of the storage ring or 3.74 μs to avoid resonance effect.

Manuscript received November 30, 1999; revised August 8, 2000. This work was supported by POSCO and MOST.

The authors are with the Pohang Accelerator Laboratory, POSTECH, Pohang, KyungBuk, 790-784, Korea (e-mail: nsh@postech.ac.kr).

Publisher Item Identifier S 0093-3813(00)11277-9.

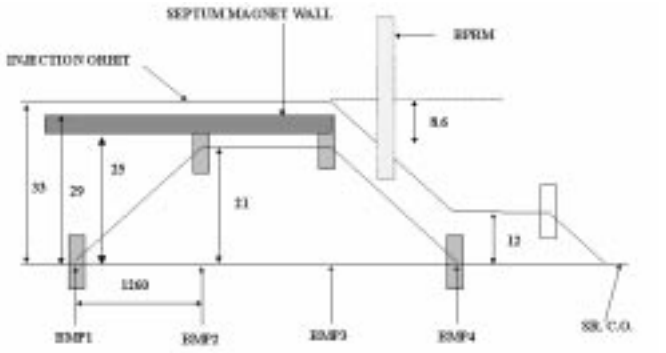

Fig. 1. Bumped beam orbit. Units are in millimeters. INJECTION: injected beam path; SR C.O.: storage ring center orbit; BPRM: beam profile screen monitor (during injection, the screen is removed); BMP1, BMP2, BMP3, BMP4: kicker magnets (1.324 kG peak field); SEPTUM MAGNET: indicates septum magnet wall (11-kG peak field).

The first two kicker magnets in Fig. 1, BMP1 and BMP2, bend the stored beam equal amounts in opposite directions, resulting in a net parallel offset of 21 mm in its beam position. The other two kicker magnets, BMP3 and BMP4, restore the beam trajectory to its original orbit. Only one kicker magnet modulator is used to drive the four kicker magnets, to give balanced current for all four magnets, and to have precise timing between magnet currents. A desirable current pulse shape is a half-sinusoid. A kicker magnet modulator that can handle a 2-GeV full energy beam is installed in the storage ring tunnel and under stable operation. In the following, design, construction, and operational experience of the kicker magnet modulator are discussed. In addition, the measurement result of spatial B-field distribution in the kicker magnet and the maximum operating range of the kicker magnet are discussed.

II. Kicker Magnet Modulator

A schematic circuit diagram of the kicker magnet modulator is shown in Fig. 2. The kicker magnet modulator is a simple series resonant circuit. The output current pulse shape is decided by the total system inductance L_t, total capacitance C_t, and system resistance R. A governing equation of the current is, when charging is V_0

$$i(t) = \frac{V_0}{\omega L_t} \cdot e^{-(R/2L_t)t} \cdot \mathrm{Sin}(\omega t) \tag{1}$$

where

$$\omega = \sqrt{\frac{1}{L_t C_t} - \frac{R^2}{4L_t^2}}.$$

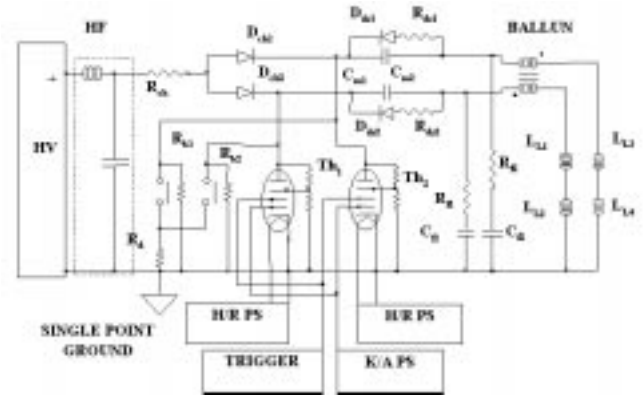

Fig. 2. Circuit diagram of kicker modulator. HV: high-voltage DC power supply (30 kV, 8 kJ/s); C_{m1}, C_{m2}: main capacitor (1.6 μF, 30 kV, 80% reversal each); L_{L1}, L_{L2}, L_{L3}, L_{L4}: kicker magnet (0.867 μH each); HF: high-frequency filter; R_{ch}: charging resistor (60 Ω); R_{b1}, R_{b2}: bleeding resistor (20 MΩ each); $D_{\rm ch1}$, $D_{\rm ch2}$: charging diode; $R_{\rm ds1}$; $R_{\rm ds2}$: discharge resistor (2 Ω each); $D_{\rm ds1}$, $D_{\rm ds2}$: discharge diode; R_{f1}; R_{f2}: surge suppression resistor (5 Ω each); $\rm Th_1$, $\rm Th_2$: EEV CX1536AX thyratron; C_{f1}; C_{f2}: surge suppression capacitor (178 nF each); R_d: dump resistor (5 kΩ).

Because the output current has a half-sinusoidal waveform, the pulsewidth of the current is approximately, by assuming a low system resistance

$$\text{Pulsewidth} \cong \pi\sqrt{L_t C_t}. \tag{2}$$

Energy per pulse can be calculated by the following formula:

$$E_0 = \tfrac{1}{2} C_t V_0^2. \tag{3}$$

Flat-top width can be calculated as follows:

$$\text{Flat} - \text{top width} = \left(\frac{T}{4} - t_{\min}\right) \times 2 \tag{4}$$

where $T = A$ period of the sinusoid and $t_{\min} =$ time to reach 99.6% of the peak current.

Specifications of the kicker magnet modulator to drive kicker magnets are given in Table I.

Major components of the modulator in Fig. 2 are a high-voltage power supply, thyratrons, and capacitors. The high-voltage DC power supply operates in a constant current charging mode. It has a maximum average output power of 8 kJ/s at 30 kV. The thyratron is an EEV CX1536A. It can handle 10-kA peak current and 250-MW peak power. As given in Table I, the required full load current at a 2-GeV operation is 24.06 kA. Because two thyratrons are used, the peak anode current required for each thyratron is 12.03 kA. Therefore, the load current required is higher than the maximum usable peak anode current of the thyratron. Because the thyratron duty is very low as given in Table I, it can handle somewhat higher current than the maximum current specified by the manufacturer. The capacity of the each main capacitor is 1.6 μF.

A charge assembly of the kicker is mainly consisted of a charging resistor (R_{ch}), charging diodes (D_{ch1}, D_{ch2}), and main capacitors (C_{m1}, C_{m2}). Energy from the HVDC power supply is charged to the main capacitor through loads $(L_{L1}, L_{L2}, L_{L3}, L_{L4})$. The main components of the kicker discharge assembly are thyratrons (Th_1, Th_2), inverse energy

TABLE I
SPECIFICATION OF KICKER MODULATOR AT 2 GeV

Parameter	Specification
Peak Current	24.06 kA
Peak Charging Voltage	16.5 kV
Pulse-Width	6.0 μs
FWHM	4.0 μs
Flat-top Width (< ±0.2%)	200 ns
Repetition Rate	10 Hz
Total System Inductance	1.17 μH
•Total Load Inductance	0.867 μH
•Total Stray Inductance	0.303 μH
Total System Capacitance	3.2 μF
Peak Energy per Pulse	435.6 Joule
Maximum Operable Beam Energy	2.0 GeV

dump assemblies (D_{ds1} and R_{ds1}, D_{ds2}, and R_{ds2}), and transient suppression assemblies (R_{f1} and C_{f1}, R_{f2}, and C_{f2}). After a charging cycle, the thyratrons are triggered simultaneously and rapidly discharge the main capacitor energy through loads. The inverse energy dump assemblies are in parallel connection with the main capacitors. A role of the inverse dump assembly is to discharge inversely charged energy on capacitors while maintaining forward charged energy. Fast discharge of the inverse energy is necessary to have a constant initial condition of main capacitors during repetitive operation and to reduce surge current of the HVDC power supply during the charging cycle. In resonant circuits, peak inverse voltage is often a problem and can be as high as the forward charging voltage. The thyratron does not allow inverse conduction, and therefore, overall inverse voltage should be blocked by the thyratron. However, peak inverse voltage of the CX1536A thyratron should be less than 10 kV for the first 25 μs. Moreover, the lifetime of capacitors strongly depends on peak inverse voltage. Thus, reduction of inverse voltage of thyratrons and capacitors within a given specification is very important in resonance circuits. To reduce the thyratron inverse voltage, it is common to use a circuit that has underdamped during the half-cycle and overdamped after the half-cycle [3]–[5]. However, this method does not sufficiently reduce the inverse voltage in our circuit. Instead of thyratrons, semiconductor switches are often used in kicker modulators to avoid the inverse voltage problem [6]–[8]. This scheme inherently does not have an inverse voltage problem because of the inverse blocking capability of semiconductor switches. But the semiconductor switch has a high-voltage limitation and is not cost effective. As shown in Fig. 2, a new scheme is developed to effectively reduce the inverse voltage by using series connected RC circuits (R_{f1} and C_{f1}, R_{f2} and C_{f2}), which are in parallel connection with the magnet loads. The energy in capacitors C_{f1} and C_{f2} maintains a continuity of the load current when the current begins to reverse. Because the load is inductive, maintaining the load current can reduce inverse voltage.

The thyratron trigger amplifier receives a pulsed optical signal via an optical fiber. The kicker modulator timing is synchronized with the PLS storage ring RF that has an operation frequency of 500 MHz. The kicker modulator is controlled with a microprocessor-based system so that it can be remotely

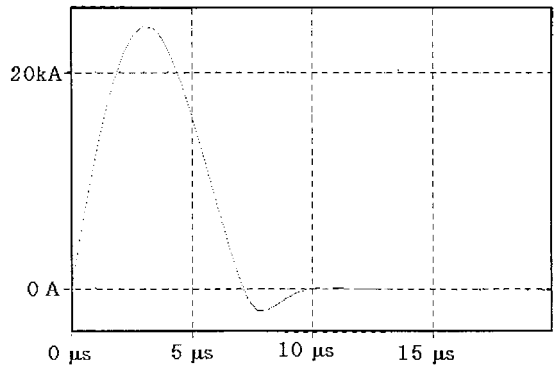

Fig. 3. Simulated total load current (16 kV charging). 24.24-kA peak, 7.1-μs pulsewidth, 4.47-μs FWHM.

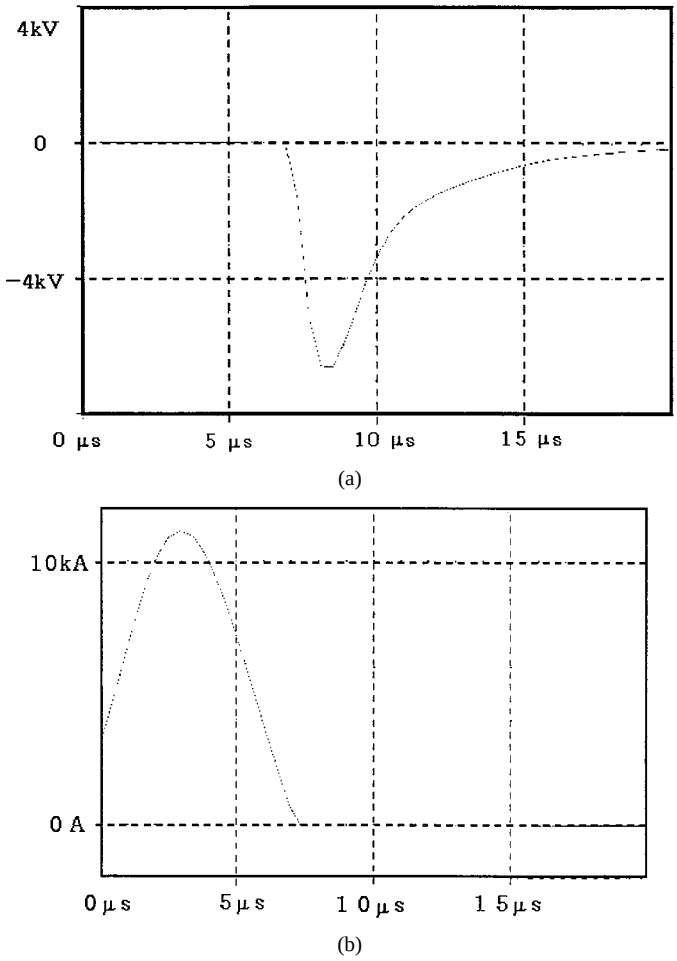

Fig. 4. Simulated thyratron inverse voltage and forward current (16 kV charging). (a) Voltage, -6.6-kV peak. (b) Current, 11.12-kA peak.

controlled from the storage ring main control room. A standard IEEE 422 is used as a main communication protocol.

III. Circuit Simulation

Spice is used for a kicker circuit simulation [9]. A load current simulated from the circuit in Fig. 2 is shown in Fig. 3. The peak load current is 24.24 kA at 2.96 μs. The charging voltage is 16.0 kV. The load current waveform is not a perfect half-sinusoid that is a desired pulse shape. The waveform shows negative swing current that has a 2.0-kA peak value at 7.75 μs. The pulsewidth

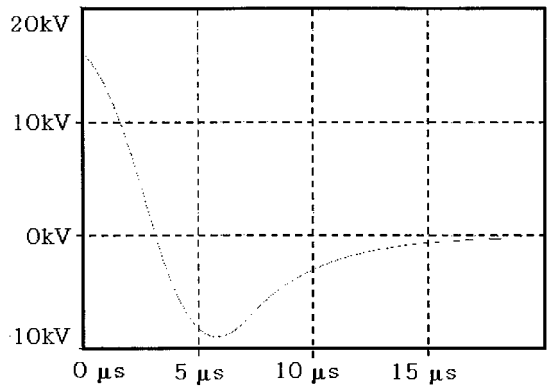

Fig. 5. Simulated main capacitor voltage (16 kV charging). -8.98-kV negative peak.

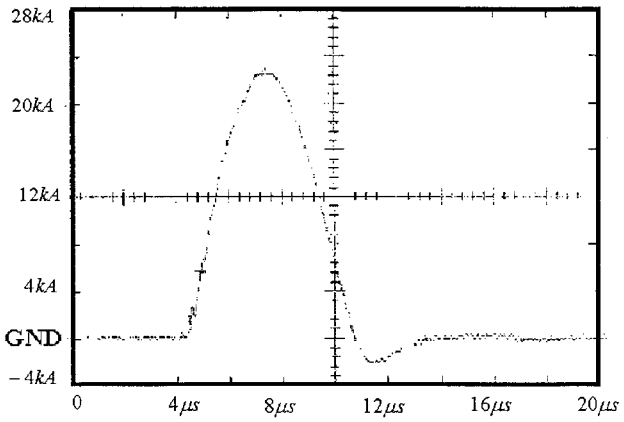

Fig. 6. Load current at 16 kV charging. 22.8-kA peak, 6.32-μs pulsewidth, 4.08-μs FWHM.

is 7.1 μs. The negative swing appears to be due to the RC transient suppression circuit (R_{f1} and C_{f1}, R_{f2} and C_{f2} in Fig. 2). The energy in the RC circuit try to keep the load current to reduce the load voltage transient as well as the thyratron inverse voltage. In Fig. 4, simulated voltage and current of the thyratron are given. The inverse voltage on thyratron starts to develop at 6.91 μs and reaches its peak value of -6.6 kV at 8.5 μs. Without the RC transient suppression circuit, the inverse voltage could be as high as the charging voltage. High inverse voltage can cause severe breakdown damage to the thyratrons. The simulation result satisfies the peak inverse voltage limitation that is less than 10 kV. As shown in Fig. 4(b), the thyratron peak current is 11.12 kA, which is slightly exceeding the maximum allowable anode peak current of 10 kA. Because the thyratron duty is very low, this overcurrent is acceptable. A voltage waveform of main capacitor (C_{m1}) is shown in Fig. 5. The peak negative voltage of capacitor is -9.0 kV, which is well within the maximum specification. The inverse energy is completely discharged in 20 μs from the beginning of a pulse. The inverse energy dump assembly (D_{ds1} and R_{ds1}, D_{ds2} and R_{ds2}) controls the discharge time of the capacitor inverse energy. Fast discharge of inverse energy also aids in reducing the inverse voltage across thyratrons and main capacitors. In addition, the fast removal of inverse energy is necessary to decrease the charging current surge of the HVDC power supply. It also gives a same initial condition of main capacitors in pulse-to-pulse operation. With a given

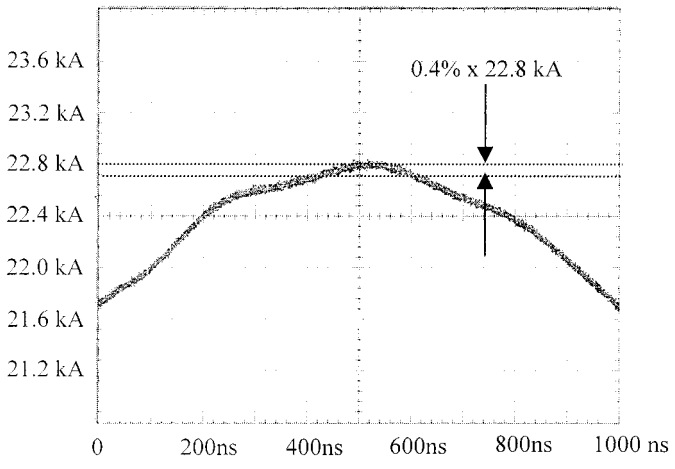

Fig. 7. An expanded view of the peak waveform shown in Fig. 6. The flat-top width measured is about 200 ns.

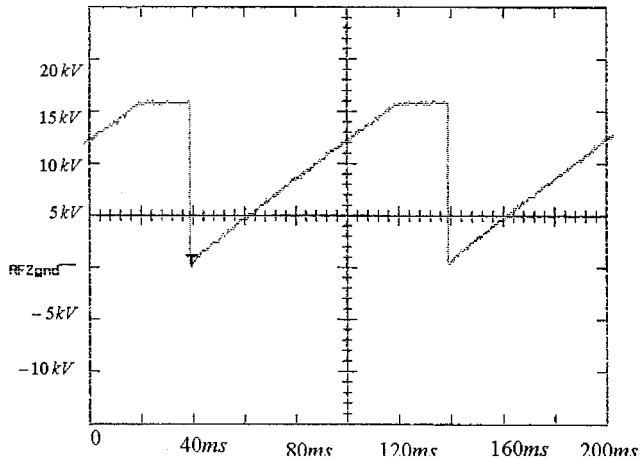

(a)

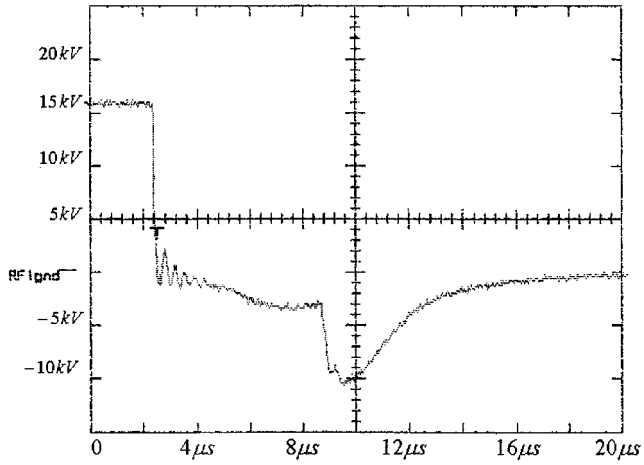

(b)

Fig. 8. Experimental result of thyratron voltage (16 kV charging). (a) Charging voltage waveform at 10-Hz operation (16-kV peak). (b) Expanded view of (a).

pulsewidth of 6 μs that corresponds to a half-period of a full sinusoid, the flat-top width can be calculated from (4) as 342 ns.

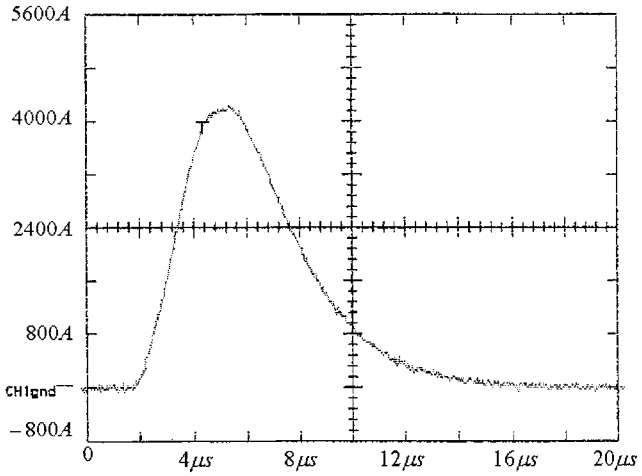

Fig. 9. Current through discharge diode: $D_{\rm ds1}$, $D_{\rm ds2}$ (4.2-kA peak).

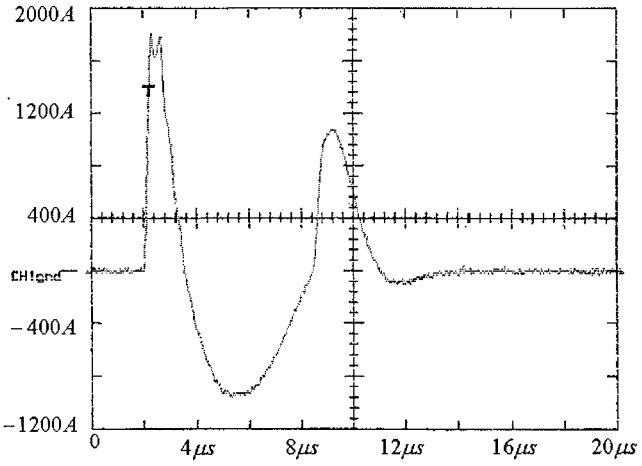

Fig. 10. Current of surge suppression capacitor: C_{f1}, C_{f2}.

IV. Experimental Results

In Fig. 6, an experimentally measured load current is displayed. The peak load current measured at 16 kV charging is 22.8 kA. The full pulsewidth measured is 6.32 μs. Full-width at half maximum (FWHM) is measured as 4.08 μs. The peak negative current is 2.2 kA at $\sim$7 μs. The result agrees very well with the simulation result shown in Fig. 4. In Fig. 7, an expanded view of the waveform given in Fig. 6 is shown to measure the flat-top width. The flat-top width measured is about 200 ns, which meets the required specification. Voltage across the thyratron is measured and given in Fig. 8. Fig. 8(a) shows the thyratron anode voltage during a 10-Hz operation. An expended view of the thyratron voltage at the moment of thyratron switching is given in Fig. 8(b). In the figure, thyratron inverse voltage can clearly be recognized. Less than a 10-kV thyratron inverse voltage is achieved as predicted from the simulation. The peak current of each diode in the inverse dump assembly $(D_{\rm ds1}, D_{\rm ds2})$ is measured as 4.2 kA. A diode current waveform is shown in Fig. 9. It can be seen from the figure that inversely charged energy is dissipated within 10 μs and initialize the energy storage capacitor for a next pulse. The peak current and the voltage of each capacitor (C_{f1}, C_{f2}) in the transient sup-

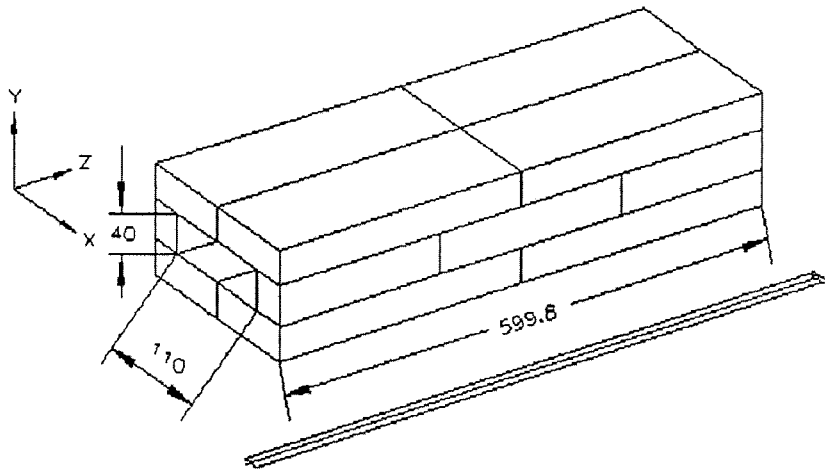

Fig. 11. Structure of the kicker magnet core.

TABLE II
SPECIFICATION OF KICKER MAGNET

Parameter	Specification
Beam Energy	2.0 GeV
Bending Field	0.1324 T
Maximum Relative Field Deviation	0.5 %
Max Jitter from Magnet to Magnet	6 ns
Number of Turns per Pole	1 turn
Resistance of Magnet @40 ℃	8.28 mΩ
Inductance of Magnet	0.867 μH
Gap Height	0.04 m
Gap Width	0.11 m
Magnet Length	0.5998 m

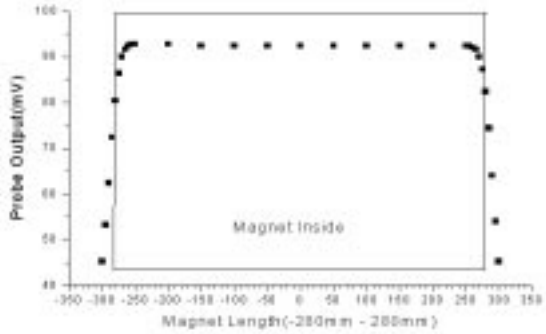

Fig. 12. Z-axis spatial magnetic field distribution in the kicker magnet.

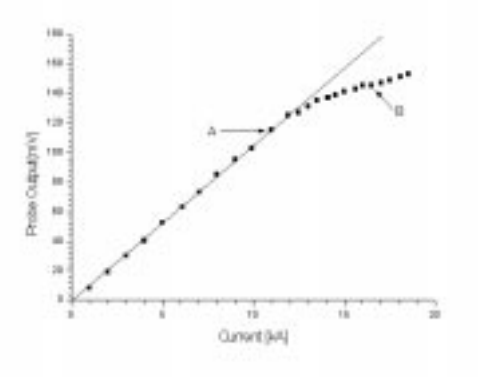

Fig. 13. Peak current versus peak magnetic flux density in the kicker magnet.

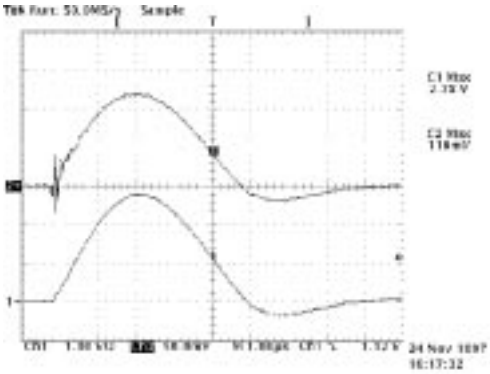

Fig. 14. Waveforms of current (bottom trace: $I = 11.12$ kA) and magnetic flux density (top trace) at point A in Fig. 12.

pression assemblies are about 1.8 kA and 10 kV, respectively. A capacitor current waveform is given in Fig. 10. The capacitor current immediately starts when the thyratron is triggered to conduct. After the capacitor is charged to a certain voltage level that is balanced with the load voltage, the capacitor starts to supply current to the load to maintain forward load current and thus suppress inverse voltage transients.

V. KICKER MAGNET

The major parameters of the kicker magnet at a 2-GeV storage ring operation are given in Table II [10]. The core material of the kicker magnet is MN-80C ferrite. Structure of the core is shown in Fig. 11. Units are in mm. The core is consisted of total 14 blocks. Each block has a thickness of 30 mm. A B-dot probe with integrator is used to measure the magnetic field. The measured result shows that the field is distributed uniformly in magnet transverse and longitudinal directions. Fig. 12 shows an example of z-axis field distribution. In Fig. 13, variation of the peak magnetic flux density is plotted as applied magnet current increases. Waveforms of current and magnetic flux density are given in Fig. 14. The waveform in Fig. 14 corresponds to the point A in Fig. 13 where the core is not saturated. The magnetic core starts to saturate around 12 kA.

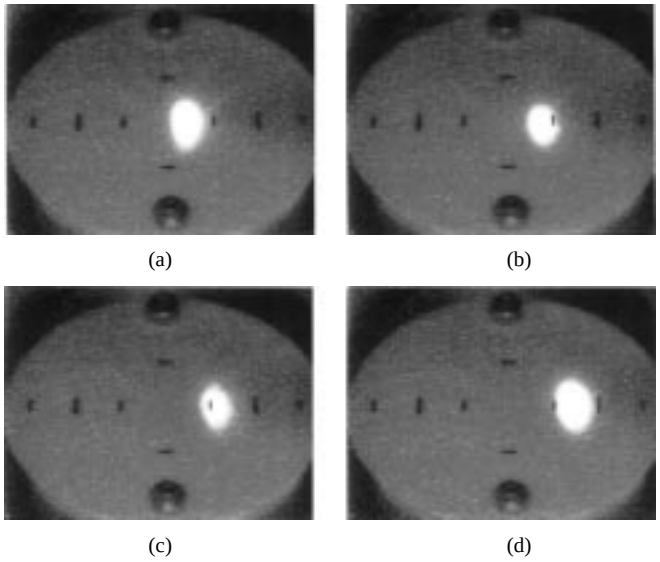

Fig. 15. Beam position observed at the beam profile monitor screen. (a) 5 kA (1.82 mm); (b) 10 kA (3.6 mm); (c) 15 kA (5.28 mm); (d) 20 kA (6.86 mm).

This magnet current corresponds to a 24-kA kicker modulator current. This maximum operable current allows 21-mm or a 16.7-mrad bump at 2 GeV. The 21-mm bump is the required specification at 2.0 GeV. Fig. 15 shows the positions of the electron beam appeared on the beam profile screen monitor as the kicker current increases from 5 kA to 20 kA at 2-GeV injection energy. Without kicker current, the beam is positioned at the center of screen. Each vertical and horizontal scale on the screen is 5 mm. As shown in Fig. 1, a 5-mm bump on BPRM corresponds to a 12.2-mm actual bump. The bump distances measured from Fig. 15 agree well with theoretically calculated values.

The injection kicker modulator was installed in August 1995. The total accumulated operation hours was 22 500 as of July 1999. Since the installation of kicker modulator, we have not detected any major faults. Any minor faults were due to strong switching noise that affects communication, control, and interlock circuits. These faults did not seriously delay overall beam injection time because they only required simple reset action to recover. Overall performance of the injection kicker modulator has been very stable and reliable.

VI. Conclusion

An injection kicker modulator is designed, constructed in house, and installed in a PLS storage ring to inject a 2.0-GeV electron beam. Specification of the kicker magnet modulator is $\sim$6.0-μs-full width, 200-ns flat-top width with $\pm$0.2% regulation, $\sim$24-kA peak current, and 10-Hz repetition rate. Two thyratron switches (EEV CX-1536AX) are used in the system. Output current waveform is a half-sinusoid. To effectively control peak inverse voltage on thyratrons and energy storage capacitors, a new type of transient suppression circuit is developed. Spatial magnetic field distribution in the kicker magnet is measured, and measurement result shows good uniformity. The maximum operable current without core saturation per each kicker magnet is found to be 12 kA, which corresponds to a 24-kA modulator current. This current satisfies a 2-GeV specification that is a 21-mm or a 16.7 mrad bump. The kicker modulator was installed in August 1995. The total accumulated operation hours was 22 500 as of July 1999. The modulator has been operated very reliably without any significant failure.

References

[1] J. Choi, T. Lee, M. Kwon, J. Y. Huang, S. H. Nam, M. Yoon, M. H. Choi, I. S. Ko, and W. Namkung, "Operational status of Pohang light source," in *Proc. Particle Accelerator Conf.*, Vancouver, B.C., Canada, 1997, p. 823.

[2] H. Winick, *Synchrotron Radiation Sources*. Singapore: World Scientific, 1994.

[3] B. E. Strickland, B. L. Thomas, G. L. Schofield, W. P. White, B. Ng, and D. Meaney, "Thyratron switched pulsed modulators for the kicker and thin septum magnets in a 1.2 GeV synchrotron radiation source," in *Proc. 8th IEEE Int. Pulsed Power Conf.*, San Diego, CA, 1991, p. 953.

[4] ——, "Fast power supplies for kicker and thin septum magnets in a 1.2 GeV synchrotron radiation source," in *Proc. Particle Accelerator Conf.*, San Fransisco, CA, 1991, p. 3171.

[5] D. Tommasini, "Injection into the elettra storage ring," in *Proc. Particle Accelerator Conf.*, Washington, DC, 1993, p. 1375.

[6] C. R. Rose and D. H. Shadel, "Design of a pulsed-current source for the injection-kicker magnet at the los alamos neutron scattering center," in *Proc. 10th IEEE Int. Pulsed Power Conf.*, Albuquerque, NM, 1995, p. 1432.

[7] R. J. Sachtschale, C. Dickey, and P. Morcombe, "A novel technique for pulsing magnet strings with a single switch," in *Proc. Particle Accelerator Conf.*, Washington, DC, 1993, p. 1339.

[8] G. Stover and L. Reginato, "Design and preliminary results for a fast bipolar resonant discharge pulser using SCR switches for driving the injection bump magnets at the ALS," in *Proc. Particle Accelerator Conf.*, Washington, DC, 1993, p. 1351.

[9] IsSpice4, Intusoft, Dan Pdero, CA, 1995.

[10] "Design Report of Pohang Light Source (revised ed.)," Pohang Accelerator Laboratory, Korea, 1992.

S. H. Nam (S'88–M'89) received the Ph.D. degree in electrical engineering from the University of South Carolina in 1990.

Since 1991, he has been with the Pohang Accelerator Laboratory (PAL), Pohang, Korea, as a Senior Researcher. During the construction of Pohang Light Source 2.5-GeV electron accelerator facility, he developed the 200-MW modulators for 80-MW klystrons, the kicker modulator, and the 60-kW, 500-MHz CW RF amplifiers. His research interests include pulsed power technology, power electronics, and high-power plasma switches. He is presently the Head of the Accelerator Department of PAL.

S. H. Jeong was born June 28, 1963, in Busan, Korea. He received the B.S. and M.S. degrees in electrical engineering from Ulsan University in 1988 and 1990, respectively.

Since 1990, he has been working as a Research Assistant at the Pohang Accelerator Laboratory of the Pohang University of Science and Technology, Pohang, Korea. His main working area is pulsed power technology and high current switching. His current interests include pulsed power technology, power electronics, and the development of pulse wire technique for the measurement undulator.